JOURNAL OF AIRCRAFT
Vol. 44, No. 4, July–August 2007

Doubly Curved Anisotropic Sandwich Panels: Modeling and Free Vibration

Terry Hause*
Minnesota State University, Mankato, Minnesota 56001
and
Liviu Librescu†
Virginia Polytechnic Institute and State University, Blacksburg, Virginia 24061-0219

DOI: 10.2514/1.26990

Problems related with the modeling and behavior in free vibration of doubly curved sandwich panels with laminated face sheets are developed in this paper. Implications of anisotropy and stacking sequence of face sheets as well as of transverse orthotropy of the core on the free vibration behavior are highlighted. Other parameters, mainly geometrical ones, are also considered in the numerical simulations, and their implications on the vibrational behavior are put into evidence. Because of the absence of similar results in the specialized literature, this paper is likely to fill a gap in the state of the art of this problem and provide pertinent results that are instrumental in the design of advanced sandwich shells.

Introduction

A CONTINUOUS interest for an extensive use of sandwich structures in the construction of advanced supersonic/hypersonic flight vehicle and resusable space transportation systems has been manifested in the last decade and is more than sure that this trend will continue and intensify in the years ahead. The works of the two last international conferences on sandwich structures [1,2] underline in full this considerable interest. A similar trend is manifested also in the naval constructions (see, e.g., [3]), and in automotive and civil engineering as well. Some of the underlying reasons and motivation for this interest emerge, among others, from

1) the possibility to integrate the advanced fiber-reinforced composite materials in the face sheets and the core, their use being likely to provide increased bending stiffness with little resultant weight penalty, long fatigue life, and directional properties of face sheets;

2) the possibility to provide thermal and sound insulation characteristics, as well as a smooth aerodynamic surface in a high-speed flow environment;

3) extended operational life as compared to stiffened-reinforced structures which are weakened by the appearance of stress concentration.

Needless to say, the development of new manufacturing techniques rendering sandwich structures economically feasible has contributed heavily to the widespread use of such structures in the aerospace industry.

One of the problems related with the *advanced* sandwich constructions that, in spite of its importance, has not received yet the attention it deserves, is that of their free vibration (see in this sense the works in [1,2], and the survey papers and the monographs on sandwich structures, [4–10]). Indeed, a good understanding of their free vibration is essential toward a reliable prediction of their dynamic response to time-dependent external excitations, prevention of the occurrence of the resonance, evaluation of their flutter instability and of their optimal design from the vibrational point of view. However, the state of the art of this problem reveals that only results related with the free vibration of *sandwich plates* have been supplied in the literature. The study presented here, devoted to the modeling and free vibration problem of doubly curved sandwich panels is intended to fill the existing gap in the specialized literature.

Presented as Paper 2107 at the 47th AIAA/ASME/ASCE/AHS/ASC Structures, Structural Dynamics, and Materials Conference, Newport, Rhode Island, 1–4 May 2006; received 2 August 2006; revision received 28 November 2006; accepted for publication 2 January 2007.

*Assistant Professor, Department of Mechanical and Civil Engineering.
†Professor, Department of Engineering Science and Mechanics.

Basic Assumptions

The global midsurface of the sandwich structure σ, selected to coincide with that of the core layer, is referred to a curvilinear and orthogonal Gaussian coordinate system x_α ($\alpha = 1, 2$). Through the thickness coordinate x_3 is considered positive when measured in the direction of the inward normal (see Fig. 1).

The uniform thickness of core is $2\bar{h}$, while those of the top and bottom faces are h'' and h', respectively. As a result, $H(\equiv 2\bar{h} + h' + h'')$ is the total thickness of the structure (see Fig. 1).

For the sake of identification, the quantities affiliated with the core layer will be marked by a superposed bar, while those associated with the lower and upper faces by single and double primes, respectively, placed on the right of the respective quantity.

Toward the modeling of doubly curved sandwich structures, the following assumptions are used:

1) the face sheets are manufactured from orthotropic material layers, the axes of orthotropy of the individual plies being not necessarily coincident with the geometrical axes x_α of the structure,

2) the material of the core layer features orthotropic properties in the transverse shear direction and, in addition, the thickness of the core layer is assumed to be much larger than those of the face sheets, that is, $2\bar{h} \gg h', h''$,

3) the theory involves the case of the *weak core* sandwich structure,

4) a perfect bonding between the face sheets and between the faces and the core is postulated,

5) the incompressibility in the transverse normal direction is postulated in both the core and the face sheets,

6) the principle of shallow shell theory is adopted,

7) due to the fact that $h', h'' \ll 2\bar{h}$, the transverse shear effects in the face sheets are discarded, and finally,

8) the rotatory inertia terms that have a marginal influence on the lowest branch of the frequency spectrum are ignored (see [10]).

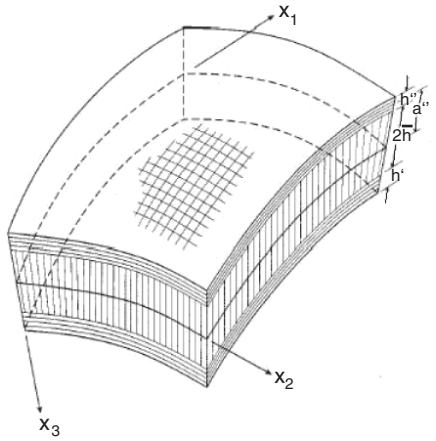

Fig. 1 Geometry of the doubly curved sandwich panel.

Kinematics

3-D Displacement Field in the Face Sheets and the Core

As a result of the previously mentioned assumptions, the 3-D distributions of the displacement field fulfilling the kinematic continuity conditions at the interfaces between the core and face sheets (see [10–13]) are represented as follows:

In the bottom face sheets ($\bar{h} \le x_3 \le \bar{h} + h'$):

$$V_1'(x_\alpha, x_3, t) = \xi_1(x_\alpha, t) + \eta_1(x_\alpha, t) - (x_3 - a)\partial v_3(x_\alpha, t)/\partial x_1 \tag{1a}$$

$$V_\alpha'(x_\alpha, x_3, t) = \xi_2(x_\alpha, t) + \eta_2(x_\alpha, t) - (x_3 - a)\partial v_3(x_\alpha, t)/\partial x_2 \tag{1b}$$

$$V_3'(x_\alpha, x_3, t) = v_3(x_\alpha, t) \tag{1c}$$

In the core ($-\bar{h} \le x_3 \le \bar{h}$):

$$\bar{V}_1(x_\alpha, x_3, t) = \xi_1(x_\alpha, t) + x_3/\bar{h}\left\{\eta_1(x_\alpha, t) + \frac{h}{2}\partial v_3(x_\alpha, t)/\partial x_1\right\} \tag{2a}$$

$$\bar{V}_2(x_\alpha, x_3, t) = \xi_2(x_\alpha, t) + x_3/\bar{h}\left\{\eta_2(x_\alpha, t) + \frac{h}{2}\partial v_3(x_\alpha, t)/\partial x_2\right\} \tag{2b}$$

$$\bar{V}_3(x_\alpha, x_3, t) = v_3(x_\alpha, t) \tag{2c}$$

In the top face sheets ($-\bar{h} - h'' \le x_3 \le -\bar{h}$):

$$V_1''(x_\alpha, x_3, t) = \xi_1(x_\alpha, t) - \eta_1(x_\alpha, t) - (x_3 + a)\partial v_3(x_2, t)/\partial x_1 \tag{3a}$$

$$V_2''(x_\alpha, x_3, t) = \xi_2(x_\alpha, t) - \eta_2(x_\alpha, t - (x_3 + a)\partial v_3(x_\alpha, t)/\partial x_2 \tag{3b}$$

$$V_3''(x_\alpha, x_3, t) = v_3(x_\alpha, t) \tag{3c}$$

In these equations, $V_i(x_\alpha, x_3, t)$ are the 3-D displacement components in the direction of the coordinate x_i, while $\xi_\alpha = (\overset{\circ}{V}{}_\alpha' + \overset{\circ}{V}{}_\alpha'')/2$ and $\eta_\alpha = (\overset{\circ}{V}{}_\alpha' + \overset{\circ}{V}{}_\alpha'')/2$ denote the average and half difference of the tangential displacements $\overset{\circ}{V}{}_\alpha'$ and $\overset{\circ}{V}{}_\alpha''$ of the points of the midsurfaces of the bottom and top face sheets, respectively.

For a symmetric sandwich panel, $h' = h'' \equiv h$ and $a' = a'' = a(\equiv \bar{h} + h/2)$ define the thickness of the bottom/top face sheets, respectively. In the previous and the remaining equations, the Greek indices have the values 1 and 2, while the Latin indices have the values 1, 2, and 3 and, unless otherwise stated, the Einstein summation convention over the repeated indices is employed.

Distribution of Strain Quantities Across the Shell Thickness

Use of Eqs. (1–3) in the 3-D strain-displacement relationships results in their 2-D counterpart. As part of these equations, the distribution of strain quantities across the structural thickness is obtained as follows:

In the bottom face sheets ($\bar{h} \le x_3 \le \bar{h} + h'$):

$$e_{11}' = \varepsilon_{11}' + (x_3 - a')\kappa_{11}' \tag{4a}$$

$$e_{22}' = \varepsilon_{22}' + (x_3 - a')\kappa_{22}' \tag{4b}$$

$$2e_{12}' = \gamma_{12}' + (x_3 - a')\kappa_{12}' \tag{4c}$$

In the soft core layer ($\bar{h} \le x_3 \le \bar{h}$):

$$2\bar{e}_{13} = \bar{\gamma}_{13} \tag{5a}$$

$$2\bar{e}_{23} = \bar{\gamma}_{23} \tag{5b}$$

and

In the top face sheets ($-\bar{h} - h'' \le x_3 \le -\bar{h}$):

$$e_{11}'' = \varepsilon_{11}'' + (x_3 + a'')\kappa_{11}'' \tag{6a}$$

$$e_{22}'' = \varepsilon_{22}'' + (x_3 + a'')\kappa_{22}'' \tag{6b}$$

$$2e_{12}'' = \gamma_{12}'' + (x_3 + a'')\kappa_{12}'' \tag{6c}$$

In these equations ε_{11}, ε_{22}, and $\varepsilon_{12}(\equiv \gamma_{12}/2)$ denote the tangential strain measures; κ_{11}, κ_{22}, and κ_{12} denote the bending strains, while $\bar{\varepsilon}_{13}(\equiv \bar{\gamma}_{13}/2)$, and $\bar{\varepsilon}_{23}(\equiv \bar{\gamma}_{23}/2)$ denote the 2-D transverse shear strain measures. Their expressions in terms of the 2-D displacement measures ξ_1, ξ_2, η_1, η_2, and v_3 are displayed in Appendix A.

Equations of Motion and Boundary Conditions

Hamilton's principle is used to derive the equations of motion and boundary conditions, (see Ref. [10]).

It is formulated as

$$\delta J = \delta \int_{t_0}^{t_1} (U - W - T)\,\mathrm{d}t = 0 \tag{7}$$

where t_0 and t_1 are two arbitrary instants of time; U denotes the strain energy; W denotes the work done by surface tractions, edge loads, and body forces; T denotes the kinetic energy of the 3-D body of the sandwich structure, while δ is the variation operator.

In Eq. (7)

$$\delta U = \frac{1}{2}\int_\sigma \left[\int_{\bar{h}}^{\bar{h}+h'} \sigma_{ij}'\delta e_{ij}' + \int_{-\bar{h}}^{+\bar{h}} \bar{\sigma}_{ij}\delta\bar{e}_{ij} + \int_{-\bar{h}-h''}^{-\bar{h}} \sigma_{ij}''\delta e_{ij}''\right]\mathrm{d}x_3\,\mathrm{d}\sigma \quad (i, j = 1, 2, 3) \tag{8}$$

where σ_{ij} denotes the stress tensor and σ denotes the midsurface area

of the sandwich panel. In addition, as a result of Hamilton's condition, $\delta V_i = 0$ at t_0, t_1 one obtains

$$\int_{t_0}^{t_1} \delta T \, \mathrm{d}t = -\int_{t_0}^{t_1} \mathrm{d}t \Bigg[\int_\sigma \int_{\bar{h}}^{\bar{h}+h'} \rho' \ddot{V}_i' \delta V_i' \, \mathrm{d}x_3 + \int_{-\bar{h}}^{\bar{h}} \bar{\rho} \ddot{\bar{V}}_i \delta \bar{V}_i \, \mathrm{d}x_3 + \int_{-\bar{h}-h''}^{-\bar{h}} \rho'' \ddot{V}_i'' \delta V_i'' \, \mathrm{d}x_3 \Bigg] \tag{9}$$

while the variation of work done by the body forces and external loads is

$$\delta W = \int_\sigma \Bigg[\int_{\bar{h}}^{\bar{h}+h'} \rho' H_i' \delta V_i' \, \mathrm{d}\sigma \, \mathrm{d}x_3 + \int_{-\bar{h}}^{\bar{h}} \bar{\rho} \bar{H}_i \delta \bar{V}_i \, \mathrm{d}\sigma \, \mathrm{d}x_3 + \int_{-\bar{h}-h''}^{-\bar{h}} \rho'' H_i'' \delta V_i'' \, \mathrm{d}\sigma \, \mathrm{d}x_3 \Bigg] + \int_{\Omega_s} \boldsymbol{\sigma}_i \delta V_i \, \mathrm{d}\Omega \tag{10}$$

In Eq. (9) the superposed dots denote time derivatives, ρ denotes the mass density, of the constituent materials, $\boldsymbol{\sigma}_i = \boldsymbol{\sigma}_{ij} n_j$ denote the components of the stress vector prescribed on the part Ω_σ of the external boundary Ω, n_i are the components of the outward unit vector normal to Ω, while H_i denote the components of the body force vector.

From Eq. (7) considered in conjunction with Eqs. (8–10), and with the strain-displacement relationships (used as subsidiary conditions) carrying out the integration with respect to x_3 and integrating by parts whenever feasible, using the expression of global stress resultants and stress couples (to be defined later) by retaining only the transversal load, transversal inertia, and transverse damping, and invoking the arbitrary and independent character of variations $\delta\eta_1$, $\delta\eta_2$, δv_3, and $\delta v_{3,n}$ throughout the entire domain of the shell and within the time interval $[t_0, t_1]$, the equations of motion and the boundary conditions of doubly curved sandwich shells are derived. By including also the effect of biaxial compressive edge loads, the obtained equations of motion are

$$\delta\xi_1\colon\ N_{11,1} + N_{12,2} = 0 \tag{11a}$$

$$\delta\xi_2\colon\ N_{22,1} + N_{12,1} = 0 \tag{11b}$$

$$\delta\eta_1\colon\ L_{11,1} + L_{12,2} - \bar{N}_{13} = 0 \tag{11c}$$

$$\delta\eta_2\colon\ L_{22,2} + L_{12,1} - \bar{N}_{23} = 0 \tag{11d}$$

$$\delta v_3\colon\ -N_{11}^0 v_{3,11} + N_{11}/R_1 - 2N_{12}^0 v_{3,12} - N_{22}^0 v_{3,22} + N_{22}/R_2 + (M_{11,11} + 2M_{12,12} + M_{22,22} + (a/\bar{h})(\bar{N}_{13,1} + \bar{N}_{23,2}) + p_3(x_\alpha, t) - C\dot{v}_3 - m_0 \ddot{v}_3 = 0 \tag{11e}$$

In Eq. (11e)

$$m_0 = \int_{-\bar{h}}^{-\bar{h}-h''} \rho_{(k)}'' \, \mathrm{d}x_3 + \int_{-\bar{h}}^{\bar{h}} \bar{\rho} \, \mathrm{d}x_3 + \int_{\bar{h}}^{\bar{h}+h'} \rho_{(k)}' \, \mathrm{d}x_3 \tag{11f}$$

denotes the mass of the structure per unit area, and C denotes the damping parameter.

Concerning the associated boundary conditions, these are

$$N_{nn} = \boldsymbol{N}_{nn}, \quad \text{or} \quad \xi_n = \boldsymbol{\xi}_n \tag{12a}$$

$$N_{nt} = \boldsymbol{N}_{nt}, \quad \text{or} \quad \xi_t = \boldsymbol{\xi}_t \tag{12b}$$

$$L_{nn} = \boldsymbol{L}_{nn}, \quad \text{or} \quad \eta_n = \boldsymbol{\eta}_n \tag{12c}$$

$$L_{nt} = \boldsymbol{L}_{nt}, \quad \text{or} \quad \eta_t = \boldsymbol{\eta}_t \tag{12d}$$

$$M_{nn} = \boldsymbol{M}_{nn}, \quad \text{or} \quad v_{3,n} = \boldsymbol{v}_{3,n} \tag{12e}$$

$$M_{nn,n} + 2M_{nt,t} + (1 + C_1/\bar{h})\bar{N}_{n3} = \boldsymbol{M}_{nt,t} + \bar{\boldsymbol{N}}_{n3} \quad \text{or} \quad v_3 = \boldsymbol{v}_3 \tag{12f}$$

In these equations, $1/R_1$ and $1/R_2$ denote the principal curvatures of the global middle surface along coordinates x_1 and x_2, respectively, considered to be constant; $(\cdot)_{,\alpha} (\equiv \partial(\cdot)/\partial x_\alpha)$ denotes the partial differentiation with respect to surface coordinate x_α; $p_3(x_\alpha, t)$ denotes the distributed transversal load to be taken into consideration in a dynamic, or when p_3 is time independent, in a static response analysis; N_{11}^0 and N_{22}^0 denote the tangential normal edge loads positive in compression, while N_{11}, N_{22}, N_{12}, $\bar{N}_{13}$, $\bar{N}_{23}$, L_{11}, L_{22}, L_{12}, and M_{11}, M_{22}, M_{12} stand for the 2-D stress resultants and stress couples. Their definition is provided in Appendix B. In addition, $C_1 = (h' + h'')/4 \longrightarrow h/2$.

The subscripts n and t in Eqs. (12) are used to designate the normal and tangential in-plane directions to an edge, implying that $n = 1$ when $t = 2$, and vice versa. The terms in bold italic denote prescribed quantities. Because of the shell curvature, the governing system will involve an inherent structural coupling between the bending and stretching motions. As a result of the six boundary conditions to be fulfilled on each panel edge, the system of governing equations should be of the order of 12.

Governing System

The governing equation system and the boundary conditions expressed in terms of the 2-D displacement measures ξ_1, ξ_2, η_1, η_2, and v_3 will be used. To this end, with the help of the 2-D versions of the constitutive equations (to be displayed in Appendix C), and strain-displacement relationships, the 2-D stress-resultant measures are expressed in terms of displacement quantities. This representation of 2-D stress resultants and stress couples replaced in the equations of motion and the boundary conditions results in the governing equations and boundary conditions in terms of displacement quantities.

In operatorial form the governing equations are as follows:

$$\mathcal{L}_{11} V_1 + \mathcal{L}_{12} V_2 + \mathcal{L}_{13} V_3 + \mathcal{L}_{14} V_4 + \mathcal{L}_{15} V_5 = 0 \tag{13a}$$

$$\mathcal{L}_{21} V_1 + \mathcal{L}_{22} V_2 + \mathcal{L}_{23} V_3 + \mathcal{L}_{24} V_4 + \mathcal{L}_{25} V_5 = 0 \tag{13b}$$

$$\mathcal{L}_{31} V_1 + \mathcal{L}_{32} V_2 + \mathcal{L}_{33} V_3 + \mathcal{L}_{34} V_4 + \mathcal{L}_{35} V_5 = 0 \tag{13c}$$

$$\mathcal{L}_{41} V_1 + \mathcal{L}_{42} V_2 + \mathcal{L}_{43} V_3 + \mathcal{L}_{44} V_4 + \mathcal{L}_{45} V_5 = 0 \tag{13d}$$

$$\mathcal{L}_{51} V_1 + \mathcal{L}_{52} V_2 + \mathcal{L}_{53} V_3 + \mathcal{L}_{54} V_4 + \mathcal{L}_{55} V_5 = p_3(x_1, x_2, t) \tag{13e}$$

where $V_i = \{\xi_1, \xi_2, \eta_1, \eta_2, v_3\}^T$ is the generalized displacement vector, while $\mathcal{L}_{ij} = \mathcal{L}_{ji}$ are 2-D partial differential operators.

In a compact form, the governing system of equations can be expressed as

$$\mathcal{L}_{ij} V_j = \mathcal{F}_i, \qquad (i, j = \overline{1,5}) \tag{14}$$

The expression of the operators is as follows:

$$\mathcal{L}_{11}(\bullet) = A_{11}\partial_{11}(\bullet) + 2A_{16}\partial_{12}(\bullet) + A_{66}\partial_{22}(\bullet) \tag{15a}$$

$$\mathcal{L}_{12}(\bullet)(=\mathcal{L}_{21}(\bullet)) = A_{26}\partial_{22}(\bullet) + A_{16}\partial_{11}(\bullet) + (A_{12} + A_{66})\partial_{12}(\bullet) \tag{15b}$$

$$\mathcal{L}_{13}(\bullet) = \mathcal{L}_{14}(\bullet)(=\mathcal{L}_{31}(\bullet) = \mathcal{L}_{41}(\bullet)) = 0 \tag{15c}$$

$$\mathcal{L}_{15}(\bullet)(=\mathcal{L}_{51}(\bullet)) = -(A_{11}/R_1 + A_{12}/R_2)\partial_1(\bullet) - (A_{16}/R_1 + A_{26}/R_2)\partial_2(\bullet) \tag{15d}$$

$$\mathcal{L}_{22}(\bullet) = A_{22}\partial_{22}(\bullet) + 2A_{26}\partial_{12}(\bullet) + A_{66}\partial_{11}(\bullet) \tag{15e}$$

$$\mathcal{L}_{23}(\bullet) = \mathcal{L}_{24}(\bullet)(=\mathcal{L}_{32}(\bullet) = \mathcal{L}_{42}(\bullet)) = 0 \tag{15f}$$

$$\mathcal{L}_{25}(\bullet)(=\mathcal{L}_{52}(\bullet)) = -(A_{22}/R_2 + A_{12}/R_1)\partial_2(\bullet) - (A_{26}/R_2 + A_{16}/R_1)\partial_1(\bullet) \tag{15g}$$

$$\mathcal{L}_{33}(\bullet) = A_{11}\partial_{11}(\bullet) + A_{66}\partial_{22}(\bullet) + 2A_{16}\partial_{12}(\bullet) - d_1 \tag{15h}$$

$$\mathcal{L}_{34}(\bullet)(=\mathcal{L}_{43}(\bullet)) = (A_{12} + A_{66})\partial_{12}(\bullet) + A_{16}\partial_{11}(\bullet) + A_{26}\partial_{22}(\bullet) \tag{15i}$$

$$\mathcal{L}_{35}(\bullet) = (\mathcal{L}_{53}(\bullet)) = -d_1 a\partial_1(\bullet) \tag{15j}$$

$$\mathcal{L}_{44}(\bullet) = A_{22}\partial_{22}(\bullet) + A_{66}\partial_{11}(\bullet) + 2A_{26}\partial_{12}(\bullet) - d_2 \tag{15k}$$

$$\mathcal{L}_{45}(\bullet)(=\mathcal{L}_{54}(\bullet)) = -d_2 a\partial_2(\bullet) \tag{15l}$$

$$\begin{aligned}\mathcal{L}_{55}(\bullet) = {} & (A_{11}/R_1^2 + A_{22}/R_2^2 + 2A_{12}/R_1R_2) - d_1a^2\partial_{11}(\bullet) \\ & - d_2a^2\partial_{22}(\bullet) + F_{11}\partial_{1111}(\bullet) + F_{22}\partial_{2222}(\bullet) + 4F_{66}\partial_{1122}(\bullet) \\ & + 2F_{12}\partial_{1122}(\bullet) + 4F_{16}\partial_{1112}(\bullet) + 4F_{26}\partial_{1222}(\bullet) + N_{11}^0\partial_{11}(\bullet) \\ & + N_{22}^0\partial_{22}(\bullet) + C/\partial_t(\bullet) + m_0\partial_{tt}(\bullet)\end{aligned} \tag{15m}$$

where the usual differentiation symbols $\partial_{ij}(\bullet) \equiv \partial^2(\bullet)/\partial x_i \partial x_j$ and $\partial_{tt}(\bullet) \equiv \partial^2(\bullet)/\partial t^2$ have been used. Concerning the load terms $\mathcal{F}_i$ appearing in Eq. (14) these are as follows:

$$\mathcal{F}_1 = \mathcal{F}_2 = \mathcal{F}_3 = \mathcal{F}_4 = 0 \quad \text{and} \quad \mathcal{F}_5 = p_3(x_1, x_2, t) \tag{16a}$$

In addition,

$$\{d_1, d_2\} = (2\bar{K}^2/\bar{h})\{\bar{G}_{13}, \bar{G}_{23}\} \tag{16b}$$

The governing equation system (13) consisting of five equations in five unknown quantities is rather general, in the sense that it can address static and dynamic problems of large classes of doubly curved shallow sandwich shells. In particular, the obtained governing system is applicable to circular cylindrical sandwich shells of both closed and open transverse cross sections. Owing to the fact that the coefficients of Eq. (13) are constants, one can use the operator methods to reduce the system of five equations to a single governing equation in terms of a displacement potential function $\phi(x_1, x_2, t)$. To this end, by assimilating Eqs. (13) to a system of algebraic equations in V_i, with coefficients represented by multiple differentiation symbols, one can extend the method developed in [14] for a simple special case. In this context, the multiple differentiations have to be considered as products of appropriate degrees of $\partial/\partial x_1$ and $\partial/\partial x_2$. In the static case, in the absence of surface loads (i.e., of the homogeneous problem), one can obtain for the potential ϕ the equation $\mathcal{D}\phi = 0$, where $\mathcal{D}(\bullet) = \det|\mathcal{L}_{ij}|$ is an operator of the order of 12.

Toward determination of $\mathcal{D}(\bullet)$, the operations involve additions, subtractions, and multiplications, and in this process, the symbols of differentiation behave as algebraic quantities provided their coefficients are constant.

One should also remark that in the case of flat sandwich panels, implying $1/R_1 = 1/R_2 = 0$, the governing system (13) exactly decouples into two independent systems, one of the fourth order in terms of displacements ξ_1 and ξ_2, associated with the stretching problem, and the other one, of the eighth order, in terms of η_1, η_2, and v_3, governing the bending problem. It should also be mentioned that the $|\mathcal{L}_{ij}|$ operator in Eqs. (13) can be seen as the Donnell–Mushtari–Vlasov extension to the case of sandwich shells, of the isotropic [15] and laminated shell [16] counterparts. It should be noticed that the symmetry of the $|\mathcal{L}_{ij}|$ operator precludes the occurrence of complex eigenvalues and ensures the orthogonality of eigenfunctions [10].

A cursory examination of Eqs. (13) enables one to remark that with the exception of the last equation that is nonhomogeneous, the first four are homogeneous. This feature is very important in the adopted solution procedure. Considering a doubly curved panel of rectangular projection on the horizontal plane ($L_1 \times L_2$), for simply supported edges, freely movable in the normal and tangential directions, the boundary conditions are as follows:

at $x_1 = 0, L_1$:

$$N_{11} = 0, \quad N_{12} = 0, \quad \eta_1 = 0, \quad \eta_2 = 0, \quad M_{11} = 0 \quad v_3 = 0 \tag{17}$$

and at $x_2 = 0, L_2$:

$$N_{22} = 0, \quad N_{12} = 0, \quad \eta_1 = 0, \quad \eta_2 = 0, \quad M_{22} = 0 \quad v_3 = 0 \tag{18}$$

In terms of the displacement quantities, the first, second, and fifth boundary conditions can be written as

$$A_{11}\xi_{1,1} + A_{12}\xi_{2,2} + A_{16}(\xi_{2,1} + \xi_{2,2}) - (A_{11}/R_1 + A_{12}/R_2)v_3(\equiv N_{11}) = 0 \tag{19a}$$

$$A_{66}(\xi_{2,1} + \xi_{1,2} + A_{26}\xi_{2,2} + A_{16}\xi_{1,1} - (A_{16}/R_1 + A_{26}/R_2)v_3(\equiv N_{12}) = 0 \tag{19b}$$

$$F_{11}v_{3,11} + F_{12}v_{3,22} + 2F_{16}v_{3,12}(\equiv M_{11}) = 0 \tag{19c}$$

$$F_{22}v_{3,22} + F_{12}v_{3,11} + 2F_{26}v_{3,12}(\equiv M_{22}) = 0 \tag{19d}$$

In these equations the global stiffness quantities are defined in Appendix C.

Solution of the Governing System

The methodology applied in [9–12] will be pursued also within this paper. First of all, the displacements $\xi_1(x_1, x_2, t)$ and $\xi_2(x_1, x_2, t)$ are represented in the form

$$\begin{Bmatrix} \xi_1(x_1, x_2, t) \\ \xi_2(x_1, x_2, t) \end{Bmatrix} = \begin{bmatrix} (F_1)_{mn} & (F_2)_{mm} \\ (G_1)_{mn} & (G_2)_{mn} \end{bmatrix} \begin{Bmatrix} \cos\lambda_m x_1 \sin\mu_n x_2 \\ \sin\lambda_m x_1 \cos\mu_n x_2 \end{Bmatrix} \exp(i\omega_{mn} - \alpha_{mn})t \tag{20}$$

where $(F_i)_{mn}$ and $(G_i)_{mn}$ are arbitrary constants to be determined, while $\lambda_m \equiv m\pi/L_1$ and $\mu_n \equiv n\pi/L_2$. We express $v_3(x_1, x_2, t)$ in Eqs. (13a) and (13b) as

$$v_3(x_1, x_2, t) = V_{mn} \sin\lambda_m x_1 \sin\mu_n x_2, \exp(i\omega_{mn} - \alpha_{mn})t \tag{21}$$

where ω_{mn} are the undamped natural frequencies, whereas α_{mn} are real constants providing a measure of damping. Using in the same equations the representation of ξ_1 and ξ_2 as given by Eq. (20), keeping in mind that in these equations the operators $\mathcal{L}_{\alpha 3}$ and $\mathcal{L}_{\alpha 4}$ are zero, and identifying the coefficients of the same trigonometric functions, one determines F_{mn} and G_{mn} that are expressed as

$$\{(F_1)_{mn}, (F_2)_{mn}, (G_1)_{mn}, (G_2)_{mn}\}^T = \{\tilde{F}_1, \tilde{F}_2, \tilde{G}_1, \tilde{G}_2\}_{mn}^T V_{mn} \tag{22}$$

In these expressions $(\tilde{F}_1, \tilde{F}_2, \tilde{G}_1, \tilde{G}_2)_{mn}^T$ is the vector of coefficients supplied in Appendix D.

Based on above representations, Eqs. (13a) and (13b) are identically fulfilled. A procedure aimed at determining $\eta_1(x_1, x_2, t)$ and $\eta_2(x_1, x_2, t)$, similar to that used to determine ξ_1 and ξ_2, is applied to Eqs. (13c) and (13d). To this end, one represents η_1 and η_2 as

$$\begin{Bmatrix} \eta_1(x_1, x_2, t) \\ \eta_2(x_1, x_2, t) \end{Bmatrix} = \begin{bmatrix} (H_1)_{mn} & (H_2)_{mm} \\ (I_1)_{mn} & (I_2)_{mn} \end{bmatrix} \begin{Bmatrix} \cos\lambda_m x_1 \sin\mu_n x_2 \\ \sin\lambda_m x_1 \cos\mu_n x_2 \end{Bmatrix} \exp(i\omega_{mn} - \alpha_{mn})t \tag{23}$$

where $(H_i)_{mn}$ and $(I_i)_{mn}$ are undetermined coefficients. Use of representations (21) and (22) in Eqs. (13c) and (13d), followed by the identification of the coefficients of the same trigonometric functions, yields the unknown coefficients that are represented as

$$\{(H_1)_{mn}, (H_2)_{mn}, (I_1)_{mn}, (I_2)_{mn}\}^T = \{\tilde{H}_1, \tilde{H}_2, \tilde{I}_1, \tilde{I}_2\}_{mn}^T V_{mn} \tag{24}$$

The elements of the vector appearing in Eq. (24) are provided in Appendix D.

In this way, the equations of motion (13a–13d) are identically fulfilled. The remaining equation that was not fulfilled is Eq. (13e). This equation as well as the boundary conditions that are not fulfilled will be satisfied in the extended Galerkin sense (see [11–13]).

To this end, one inserts in the Hamilton's principle the representations of displacement quantities, carry out the indicated operations, and bearing in mind that the first four equations of equilibrium as well as the geometric boundary conditions are identically fulfilled, one obtains the characteristic equation as

$$S_{mn}^2 + 2\Delta_{mn}\omega_{mn}S_{mn} + \omega_{mn}^2 = 0 \tag{25a}$$

where

$$\omega_{mn}^2 = K_{mn}/m_0 \quad \text{and} \quad \Delta_{mn} = C/(2m_0\omega_{mn}) \tag{25b}$$

denote the undamped natural frequencies squared and the modal damping, respectively.

For the doubly curved sandwich panels, a dimensionless closed-form expression of undamped natural frequencies was obtained as

$$\begin{aligned} \Omega_{mn}^2 \left(\equiv \frac{m_0 L_1^4}{\pi^4 F_{11}} \omega_{mn}^2 \right) &= m^4 + \frac{F_{22} n^4 \phi^4}{F_{11}} + \frac{2(F_{12} + 2F_{66}) m^2 n^2 \phi^2}{F_{11}} \\ &+ \frac{a^2 L_1^2}{F_{11}\pi^2}(d_1 m^2 + d^2 n^2 \phi^2) + \frac{a L_1^3}{F_{11}\pi^3}[d_1 m(\tilde{H}_1)_{mn} \\ &+ d_2 n\phi(\tilde{I}_2)_{mn}] + \frac{L_1^2}{F_{11}\pi^3}[m(\psi_1 A_{11} + \psi_2 \phi A_{12})(\tilde{F}_1)_{mn} \\ &+ n\phi(\psi_1 A_{12} + \psi_2 \phi A_{22})(\tilde{G}_2)_{mn} + (n\phi(\tilde{F}_2)_{mn} \\ &+ m(\tilde{G}_1)_{mn})(\psi_1 A_{16} + \phi\psi_2 A_{26})] + \frac{L_1^2}{F_{11}\pi^4}(\psi_1^2 A_{11} + \psi_2^2 \phi^2 A_{22} \\ &+ 2A_{12}\psi_1\psi_2\phi) - K_x(m^2\psi^2 + L_R n^2 \psi^2 \phi^2) \end{aligned} \tag{26}$$

Herein $\psi_1 = L_1/R_1$, $\psi_2 = L_2/R_2$, $\phi = L_1/L_2$, $K_x = L_1^2 N_{11}^0/\pi^4 F_{11}$, and $L_R = N_{22}^0/N_{11}^0$, while the expressions of $(\tilde{H}_1)_{mn}$, $(\tilde{I}_2)_{mn}$, $(\tilde{F}_\alpha)_{mn}$, and $(\tilde{G}_\alpha)_{mn}$ are supplied in Appendix D.

Numerical Simulations

Solution Validation

Before carrying out a numerical analysis enabling one to highlight the influence played by a number of essential parameters proper to anisotropic sandwich structures, a validation of the analytical predictions obtained as per the present structural model against those available in the literature is in order. Having in view the nonexistence in the published literature of results on the free vibration problem of *curved* sandwich panels, here, the comparisons will involve flat sandwich panels only. To this end, the case of a three-layer rectangular sandwich panel $L_1 = 1.828$ m, $L_2 = 1.219$ m) whose faces are of aluminum and the core of aluminum honeycomb is

Table 1 Material and geometric characteristics

	Thickness, m	Elastic modulus, GPa	Poisson's ratio	Mass density, kg/m^3	Shear modulus, GPa	
Upper face	0.00041	68.9	0.33	3721	25.902	
Lower face	0.00041	68.9	0.33	3721	$\bar{G}_{13}$	$\bar{G}_{23}$
Core	0.0064	0	0	0	134.5, MPa	51.7, MPa

Table 2 Comparison of eigenfrequency (validation no. 1)

ω_{ij}, Hz	Experiment [17]	Exact [17]	FEM [18]	SFPM [19]	Present
$\omega_1(=\omega_{11})$	——	23	23	23.30	23.40
$\omega_2(=\omega_{21})$	45	44	44	44.48	44.64
$\omega_3(=\omega_{12})$	69	71	70	71.36	71.51
$\omega_4(=\omega_{31})$	78	80	80	78.81	79.27
$\omega_5(=\omega_{22})$	92	91	90	91.90	92.2
$\omega_6(=\omega_{32})$	125	126	125	125.16	125.97

Table 3 Comparison of eigenfrequencies ω_{mn} (Hz) for a flat sandwich panel (validation no. 2)

m	n					
	1	2	3	4	5	
1	23.5	71.0	146.5	245.3	362.5	Present study
	23.4	70.7	145.8	244.4	361.7	Hohe, Librescu, and Oh [20]
		69.0	152.0	246.0	381.0	Raville and Ueng [17] (exp)
	23.0	71.0	146.0	244.0	360.0	Raville and Ueng [17] (numerical)
2	45.1	92.1	166.7	264.5		Present study
	44.8	91.5	165.9	263.5		Hohe, Librescu, and Oh [20]
	45.0	92.0	169.0	262.0		Raville and Ueng [17] (exp)
	45.0	91.0	165.0	263.0		Raville and Ueng [17] (numerical)
3	80.7	126.8	200.1			Present study
	80.3	126.1	199.1			Hohe, Librescu, and Oh [20]
	78.0	129.0	199.0			Raville and Ueng [17] (exp)
	80.0	126.0	195.0			Raville and Ueng [17] (numerical)
4	130.0	174.9				Present study
	129.3	173.9				Hohe, Librescu, and Oh [20]
	133.0	177.0				Raville and Ueng [17] (exp)
	129.0	174.0				Raville and Ueng [17] (numerical)

considered. Their geometric and elastic characteristics are displayed in Table 1.

The various mode eigenfrequencies obtained in [17] via experiments and via an exact approach, in [18] via the finite element method (FEM), and in [19] via the spline finite point method (SFPM) are compared with those derived via the present closed-form solution, Eq. (26). The results are summarized in Table 2.

The results reveal an excellent agreement of the actual predictions with those obtained by various methods.

In addition, for the same case identified by the data supplied in Table 1, comparisons with predictions presented in [17,20] are listed in Table 3. Notice that in contrast to the present sandwich model, that of [20] includes the effect of transverse normal compressibility of the core. The compared results reveal also perfect agreement.

Following the validation of both the structural model and of the solution methodology, numerical simulations highlighting the implications of various effects on eigenfrequencies will be displayed.

Numerical Results

The material properties for the face sheets used in the forthcoming simulations are listed in Table 4. Concerning the material properties of the core, these correspond to a honeycomb titanium and are $G_{13} = 1.44$ GPa and $G_{23} = 0.651$ GPa. In addition, unless otherwise stated, $L_1 = 0.6096$ m, $\bar{h} = 0.0127$ m, $h = 0.127 \times 10^{-3}$ m, $\phi = 1$, the faces are assumed to be made up from material $F1$, and undamped vibrations are considered.

The issue of the effect of the directional property of the material of face sheets on the eigenfrequency ratio $\Omega_r \equiv \omega_{11}|_{\text{shell}}/\omega_{11}|_{\text{plate}}$ is addressed in various context in the next figures.

In Fig. 2, the effect of the ply angle of face sheets of a circular cylindrical panel ($L_2/R_2 = 0$), for various curvature ratios L_1/R_1 on eigenfrequency ratio Ω_r is displayed. In this case, as indicated in the inset of the figure, the stacking sequence of the sandwich panel is $[\theta/\text{core}/\theta]$.

It clearly appears that with the increase of L_1/R_1, the increase of the ply angle until $\theta = \pi/2$ is accompanied by the increase of Ω_r. The results also reveal that Ω_r is always larger than 1, implying that $\omega_{11}|_{\text{shell}} > \omega_{11}|_{\text{plate}}$.

In contrast to this trend, for the case of the face sheets made up of the material F2 that features a very low orthotropicity ratio, the results not displayed here reveal that the trend emerging from Fig. 2 is replaced by another one, characterized by a rather reduced sensitivity of the variation of Ω_r with that of θ. The same comment, namely, that $\Omega_r > 1$, emerges also in this case.

In Fig. 3, for a circular cylindrical panel ($L_1/R_1 = 0.4$, $L_2/R_2 = 0$), the effects of the ply angle of the material of the face sheets coupled with that of the panel aspect ratio L_1/L_2 on Ω_r are highlighted. It is seen that with the decrease of L_1/L_2 a shift of the maximum of the frequency ratio Ω_r toward larger θ is experienced, the opposite trend appears to be valid when L_1/L_2 increases in its values.

In Fig. 4, for a doubly curved panel, the implications of the variation of the ply angle for various values of L_1/R_1 are supplied. It is seen that with the increase of θ and with that of L_1/R_1, a continuous increase of the frequency parameter $(\Omega_{11})^{1/2} \equiv (m_0 L_1^4/\pi^4 F_{11})^{1/4}(\omega_{11})^{1/2}$ is resulting. It is also seen that for doubly curved shells of negative Gaussian curvature (that is for the case of $1/R_1R_2 < 0$), a decay of eigenfrequencies as compared to the zero and positive Gaussian curvature shell counterparts is experienced.

Table 4 Material properties for the face sheets

Type	Material	E_1, GPa	E_2, GPa	G_{12}, GPa	ν_{12}
F1	HS graphite epoxy	180.99	10.34	7.24	0.28
F2	IM7/977-2	79.98	75.15	9.65	0.06

Table 5 Comparison of the fundamental eigenfrequency and the critical buckling load for a plate and a shell for the layup $[\theta/-\theta/\theta/\text{Core}/\theta/-\theta/\theta]$

			Plate [13]			Shell (Fig. 11)		
θ, deg	ϕ	L_1, in. (m)	K_{cr}	N_{11}^0, lb/in. (MN/m)	$\sqrt{\Omega_{11}}$	K_{cr}	N_{11}^0, lb/in. (MN/m)	$\sqrt{\Omega_{11}}$
47	1.11	24(0.6096)	7110.28	11,866.34(2.08)	16.2771	8946.94	14,911.40(2.61)	18.7631
44.1	1.0	24(0.6096)	4913.96	9,558.94(1.67)	14.84	6945.93	13,511.65(2.37)	17.5176
38.6	0.83	24(0.6096)	2734.11	6945.17(1.22)	12.8168	4674.68	11,874.59(2.08)	14.6559
31.5	0.71	24(0.6096)	1664.60	5649.53(0.99)	11.3215	2289.93	7,771.86(1.36)	12.2611
19.8	0.62	24(0.6096)	1056.09	5048.27(0.88)	10.1042	1256.84	6007.88(1.05)	10.5534

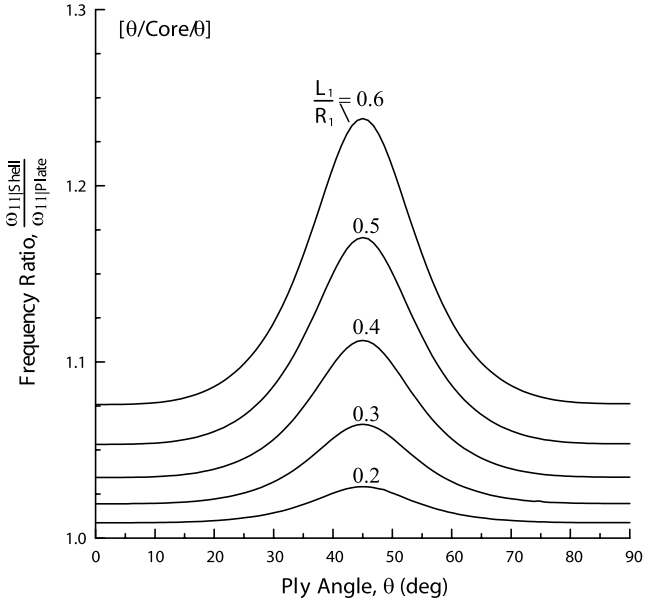

Fig. 2 Variation of the frequency ratio $\Omega_r(\equiv \omega_{11}|_{\text{shell}}/\omega_{11}|_{\text{plate}})$ vs the ply angle for a circular sandwich panel ($L_2/R_2 = 0$) for selected values of L_1/R_1.

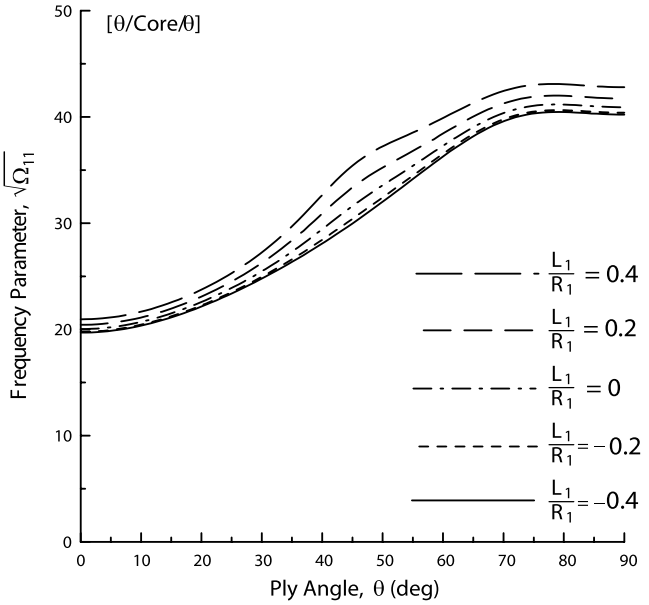

Fig. 4 Variation of the frequency parameter $(\Omega_{11})^{1/2}$ for a doubly curved panel vs θ for selected values of L_1/R_1 ($L_2/R_2 = 0.4$).

This trend is consistent with that reported in [16,21] in the case of standard laminated shells.

In Fig. 5 the implications on $\Omega_{11}^{1/2}$ of the variation of the ply angle in conjunction with that of the thickness ratio $\bar{h}/h$ for the case of a circular cylindrical panel, characterized by various values of the curvature ratios L_1/R_1, are presented. From this figure one can conclude that the increase of $\bar{h}$ yields an increase of the fundamental eigenfrequency, a trend that becomes steeper with the increase of the ply angle.

Also, Fig. 6 reveals that with the increase of $\bar{h}$, for arbitrary ply angles, the differences between plates and shells, in terms of the frequency parameter $(\Omega_{11})^{1/2}$, start to decay. A similar conclusion emerges also from Fig. 7, where the results also reveal that with the increase of $\bar{h}$, there is a lower sensitivity of $(\Omega_{11})^{1/2}$ to the variation of L_1/R_1 as compared to the case of lower $\bar{h}$.

Figure 8 presents the variation of Ω_r with the curvature ratio L_1/R_1 for selected ply angles. The results of this plot are consistent with those in Fig. 2, in the sense of the symmetry with respect to the ply angle $\theta = 45$ deg, at which value the maximum fundamental eigenfrequency is obtained.

Figure 9 shows the variation of the fundamental eigenfrequency ratio Ω_r against the aspect ratio L_1/L_2 of a circular cylindrical panel, for selected values of θ.

The results reveal in a different form what was shown in Fig. 3, namely, that the maximum of Ω_r is obtained for $L_1/L_2 = 1$ and $\theta = 45$ deg, and for $\theta = 0$ the maximum is reached when $L_1/L_2 = 2$, while for $\theta = 90$ deg, $L_1/L_2 = 0.5$

For the case of a spherical cap, the effect of the orthotropicity ratio E_2/E_1 of the material of face sheets on $\Omega_{11}^{1/2}$ is highlighted in Fig. 10. The supplied results reveal that for the material of the face sheets considered here, the ply angle has to be selected properly as to get the highest increase of the eigenfrequency.

Figure 11 highlights the values of uniaxial buckling loads, obtained for such values of $K_x(\equiv L_1^2 N_{11}^0/\pi^4 F_{11})$ for which the

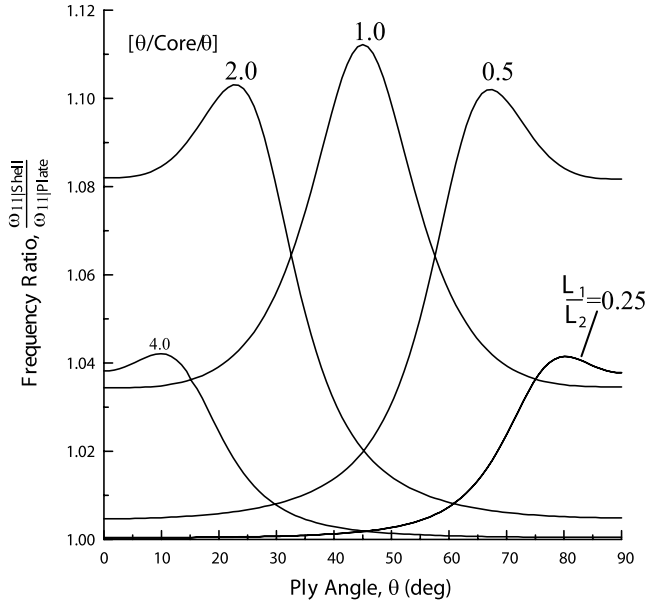

Fig. 3 Variation of Ω_r vs θ, for selected values of $\phi(=L_1/L_2)$, $L_1/R_1 = 0.4$; $L_2/R_2 = 0$.

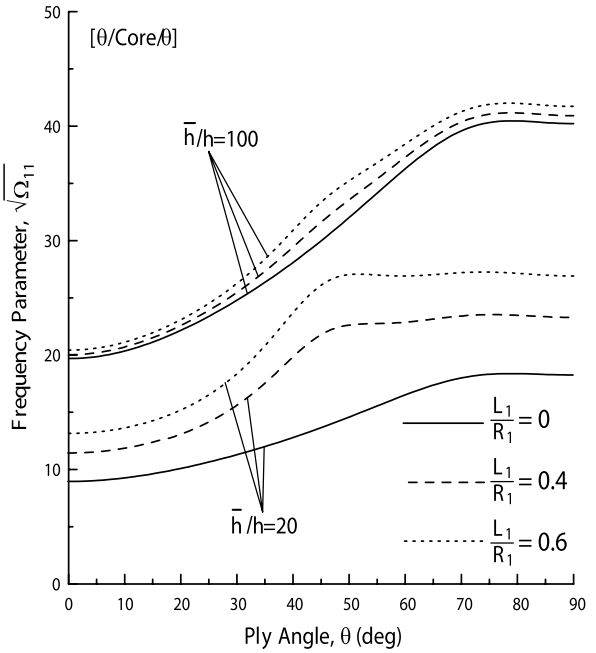

Fig. 5 Variation of $(\Omega_{11})^{1/2}$ vs θ for a circular cylindrical panel, for selected values of $\bar{h}/h$ and L_1/R_1. Herein only $\bar{h}$ varies ($L_2/R_2 = 0$).

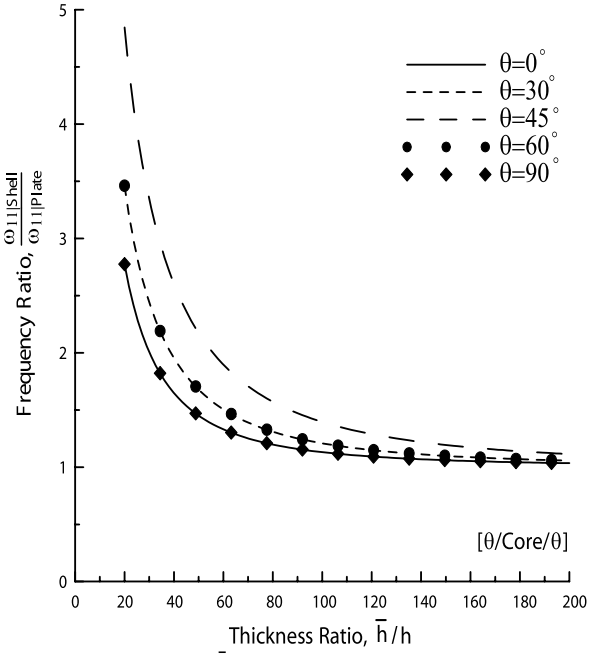

Fig. 6 Variation of Ω_r vs $\bar{h}/h$ for a spherical cap and selected values of θ. Herein, only $\bar{h}$ varies ($L_1/R_1 = 0.4, L_2/R_2 = 0.4$).

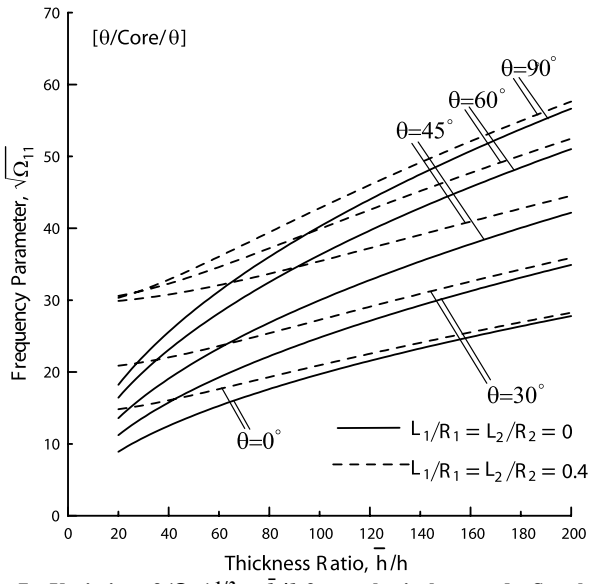

Fig. 7 Variation of $(\Omega_{11})^{1/2}$ vs $\bar{h}/h$ for a spherical cap and a flat plate, and for selected ply angles. Herein, only $\bar{h}$ varies.

frequencies vanish. The results reveal the beneficial effect played by the ply angle toward the increase of the buckling load K_{cr}.

Finally, in Table 5, there are displayed, for the case of plates and shell counterparts, the coupled effects of the ply angle and panel aspect ratio on eigenfrequency and reduced buckling load.

Some of the conclusions previously emphasized, related to the ply angle, panel aspect ratio, and curvature emerge also from this table.

Conclusions

A structural model and analytical study of the free vibration of doubly curved sandwich panels featuring laminated anisotropic face sheets have been presented. The closed-form solution obtained via implementation of the extended Galerkin solution methodology has enabled one to highlight the implications of a number of effects, such as the orthotropicity ratio of the material of face sheets and core layer,

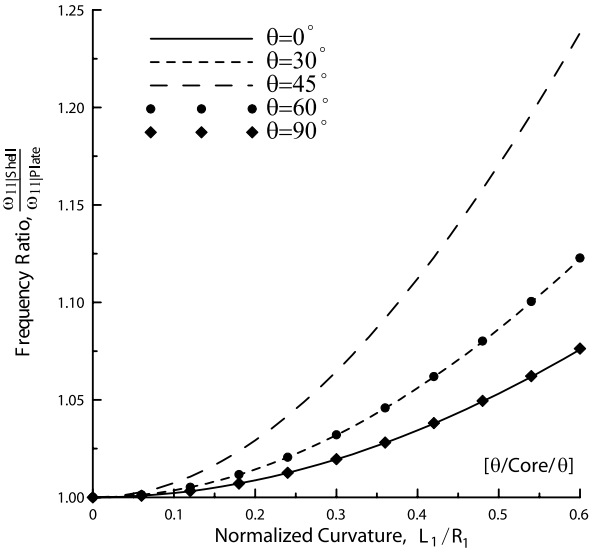

Fig. 8 Variation of Ω_r vs L_1/R_1 for a circular cylindrical shell ($L_2/R_2 = 0$), and selected values of θ ($L_1/R_1 = 0.4, L_2/R_2 = 0$).

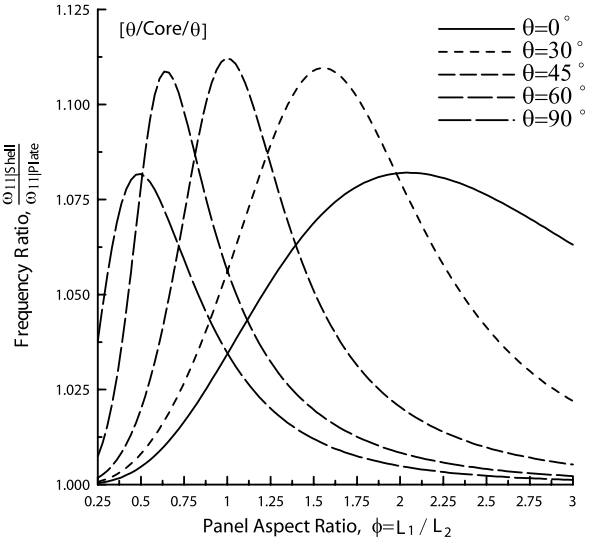

Fig. 9 Variation of Ω_r vs L_1/L_2 for a circular cylindrical panel and selected values of θ ($L_1/R_1 = 0.4, L_2/R_2 = 0$).

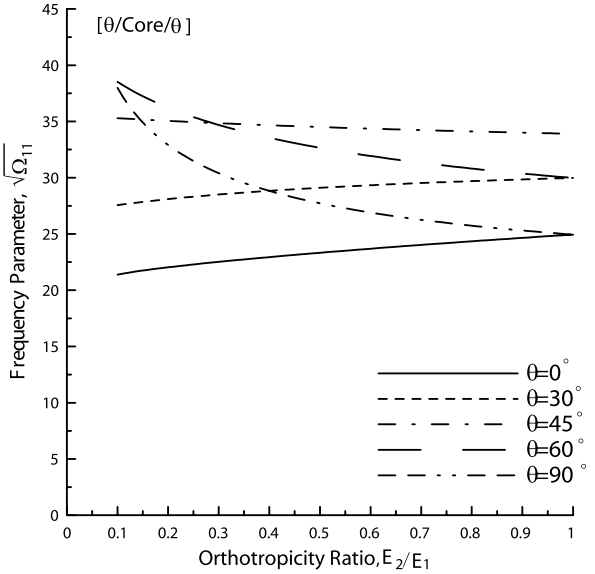

Fig. 10 Variation of $(\Omega_{11})^{1/2}$ vs E_1/E_2 for a spherical cap ($L_1/R_1 = L_2/R_2 = 0.4$), and for selected values of θ.

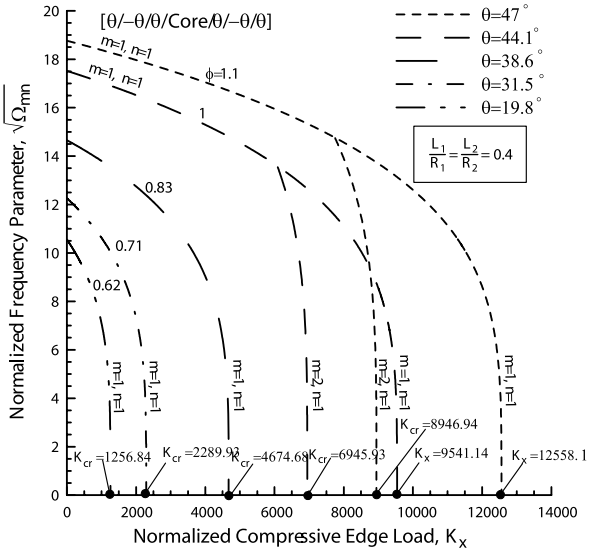

Fig. 11 Variation of $(\Omega_{mn})^{1/2}$ vs θ angles, for various mode numbers, spherical cap.

the ply angle of the material of the faces, the structural layup, the panel aspect ratio, and compressive/tensile edge loads.

Moreover, the adopted solution methodology was validated against predictions obtained via experimental, analytical, and numerical methods, and an excellent agreement was obtained.

The results have revealed the considerable potential beneficial role played by the directional property of the face sheets material, of their layup, as well as of the transverse shear orthotropicity ratio of the core material, toward the enhancement, without weight penalties, of the vibrational behavior of sandwich panels.

Having in view the scarcity of available results in the specialized literature on free vibration of sandwich shells, this paper is likely to fill a gap in the state of the art of this problem.

Appendix A

Strain-displacement relationships in the face sheets and the core layer are as follows:

Bottom face sheets:

$$\varepsilon'_{11} = \xi_{1,1} + \eta_{1,1} - v_3/R_1 \qquad (1 \rightleftarrows 2) \tag{A1a}$$

$$\gamma'_{12} = \xi_{1,2} + \xi_{2,1} + \eta_{1,2} + \eta_{2,1} \tag{A1b}$$

$$\kappa'_{11} = -v_{3,11} \qquad (1 \rightleftarrows 2) \tag{A1c}$$

$$\kappa'_{12} = -2v_{3,12} \tag{A1d}$$

Soft core layer:

$$\bar{\gamma}_{13} = \frac{1}{\bar{h}}\left\{\eta_1 + \frac{1}{2}hv_{3,1}\right\} + v_{3,1} \qquad (1 \rightleftarrows 2) \tag{A2}$$

Top face sheets:

$$\varepsilon''_{11} = \xi_{1,1} - \eta_{1,1} - v_3/R_1 \qquad (1 \rightleftarrows 2) \tag{A3a}$$

$$\gamma''_{12} = \xi_{1,2,} + \xi_{2,1} - \eta_{1,2} - \eta_{2,1} \tag{A3b}$$

$$\kappa''_{11} = -v_{3,11} \qquad (1 \rightleftarrows 2) \tag{A3c}$$

$$\kappa''_{12} = -2v_{3,12} \tag{A3d}$$

The sign $(1 \rightleftarrows 2)$ indicates that in Eqs. (A1–A3) the expressions not explicitly supplied can be obtained from the ones displayed above, upon replacing subscript 1 by 2 and vice versa. The same convention is used throughout the paper.

Appendix B

Expressions of the global stress resultants and stress couples:

$$N_{11} = N'_{11} + N''_{11} \qquad (1 \rightleftarrows 2) \tag{B1a}$$

$$N_{12} = N'_{12} + N''_{12} \tag{B1b}$$

$$L_{11} = \bar{h}(N'_{11} - N''_{11},) \qquad (1 \rightleftarrows 2) \tag{B1c}$$

$$L_{12} = \bar{h}(N'_{12} - N''_{12},) \tag{B1d}$$

$$M_{11} = M'_{11} + M''_{11} \qquad (1 \rightleftarrows 2) \tag{B1e}$$

$$M_{12} = M'_{12} + M''_{12} \tag{B1f}$$

In Eqs. (B1), the stress resultants and stress couples associated with the bottom face sheets are expressed for the shallow shell theory as

$$\left\{N'_{\alpha\beta}, M'_{\alpha\beta}\right\} = \sum_{k=1}^{N}\int_{(x_3)_{k-1}}^{(x_3)_k} (\sigma'_{\alpha\beta})_k\{1, x_3 - a'\}\,\mathrm{d}x_3, \qquad (\alpha, \beta = 1, 2) \tag{B2}$$

while the transverse shear stress measures in the core are defined as

$$\bar{N}_{\alpha 3} = \int_{-\bar{h}}^{\bar{h}} \bar{\sigma}_{\alpha 3}\,\mathrm{d}x_3 \tag{B3}$$

In the above equations, σ_{ij} are the components of the stress tensor.

The stress resultants and stress couples for the upper face can be obtained from Eqs. (B2) by replacing single primes by double primes, a' by $-a''$, where, for the present case, $a' = a'' = a$. Herein, N is the number of constituent layers in the bottom face sheets, equal with that in the upper face sheets, while $(x_3)_k$ and $(x_3)_{k-1}$ denote the distances from the global reference plane (coinciding with that of the core layer) to the upper and bottom interfaces of the kth layer, respectively.

Appendix C

2-D constitutive equations:

Having in mind that the top and bottom face sheets are symmetric with respect to both their midplanes and with the midplane of the entire structure, considering that the materials of the face sheets exhibit monoclinic symmetry and that the core material is orthotropic, one obtain the constitutive equations. These equations associated with the bottom face sheets reduced to the midplane of the structure are expressed in matrix form as

$$\begin{Bmatrix} N'_{11} \\ N'_{22} \\ N'_{12} \\ M'_{11} \\ M'_{22} \\ M'_{12} \end{Bmatrix} = \begin{bmatrix} A'_{11} & A'_{12} & A'_{16} & E'_{11} & E'_{12} & E'_{16} \\ A'_{21} & A'_{22} & A'_{26} & E'_{21} & E'_{22} & E'_{26} \\ A'_{16} & A'_{26} & A'_{66} & E'_{16} & E'_{26} & E'_{66} \\ E'_{11} & E'_{12} & E'_{16} & F'_{11} & F'_{12} & F'_{16} \\ E'_{21} & E'_{22} & E'_{26} & F'_{21} & F'_{22} & F'_{26} \\ E'_{16} & E'_{26} & E'_{66} & F'_{16} & F'_{26} & F'_{66} \end{bmatrix} \begin{Bmatrix} \varepsilon'_{11} \\ \varepsilon'_{22} \\ \gamma'_{12} \\ \kappa'_{11} \\ \kappa'_{22} \\ \kappa'_{12} \end{Bmatrix} \tag{C1}$$

The stiffness quantities appearing in Eq. (18) are defined as

$$\{A'_{\omega\rho}, D'_{\omega\rho}\} = \{A''_{\omega\rho}, D''_{\omega\rho}\} = \sum_{k=1}^{N}\int_{(x_3)_{k-1}}^{(x_3)k} (\hat{Q}'_{\omega\rho})_{(k)}(1, x_3^2)\,\mathrm{d}x_3 \tag{C2}$$

$$(\omega, \rho = 1, 2, 6)$$

where $\hat{Q}_{ij} = Q_{ij} - (Q_{i3}Q_{j3}/Q_{33})$ denotes the reduced elastic moduli, where for a symmetric construction, $\hat{Q}'_{\omega\rho} = \hat{Q}''_{\omega\rho}$ while

$$E'_{\omega\rho} = a'A'_{\omega\rho} = -E''_{\omega\rho}, \qquad F'_{\omega\rho} = D'_{\omega\rho} + a'^2 A'_{\omega\rho} = F''_{\omega\rho} \equiv F_{\omega\rho} \tag{C3}$$

The expression of stress resultants and stress couples for the upper face can be obtained from their counterparts associated with the bottom face sheets, by replacing the single prime by double primes.

For the weak core layer considered as an orthotropic body (the axes of orthotropy coinciding with the geometrical axes), the constitutive equations are

$$\bar{N}_{13} = 2\bar{h}\bar{K}^2\bar{Q}_{55}\bar{\gamma}_{13}, \qquad \bar{N}_{23} = 2\bar{h}\bar{K}^2\bar{Q}_{44}\bar{\gamma}_{23} \tag{C4}$$

where $\bar{K}^2$ is the shear transverse correction factor, while $\bar{Q}_{55}(\equiv \bar{Q}_{13})$ and $\bar{Q}_{44}(\equiv \bar{G}_{23})$ are the transverse shear moduli of the core material.

Appendix D

Expression of the terms appearing in Eqs. (22) and (23):

$(\tilde{F}_1)_{mn}$, $(\tilde{F}_2)_{mn}$, $(\tilde{G}_1)_{mn}$, and $(\tilde{G}_2)_{mn}$ are obtainable as the solution of the matrix equation

$$\begin{bmatrix} (P_{11})_{mn} & (P_{12})_{mn} & (P_{13})_{mn} & (P_{14})_{mn} \\ (P_{12})_{mn} & (P_{11})_{mn} & (P_{14})_{mn} & (P_{13})_{mn} \\ (P_{13})_{mn} & (P_{14})_{mn} & (P_{33})_{mn} & (P_{34})_{mn} \\ (P_{14})_{mn} & (P_{13})_{mn} & (P_{34})_{mn} & (P_{33})_{mn} \end{bmatrix} \begin{Bmatrix} (\tilde{F}_1)_{mn} \\ (\tilde{F}_2)_{mn} \\ (\tilde{G}_1)_{mn} \\ (\tilde{G}_2)_{mn} \end{Bmatrix} = \begin{Bmatrix} (S_1)_{mn} \\ (S_2)_{mn} \\ (S_3)_{mn} \\ (S_4)_{mn} \end{Bmatrix} \tag{D1}$$

where

$$\begin{aligned} (P_{11})_{mn} &= A_{11}m^2 + A_{66}n^2\phi^2 & (P_{12})_{mn} &= 2A_{16}mn\phi \\ (P_{13})_{mn} &= A_{16}m^2 + A_{26}n^2\phi^2 & (P_{14})_{mn} &= (A_{12} + A_{66})mn\phi \\ (P_{33})_{mn} &= A_{22}n^2\phi^2 + A_{66}m^2 & (P_{34})_{mn} &= 2A_{26}mn\phi \end{aligned} \tag{D2}$$

and

$$\begin{aligned} (S_1)_{mn} &= -\frac{m}{\pi}(\psi_1 A_{16} + \psi_2\phi A_{12}) \\ (S_2)_{mn} &= -\frac{n\phi}{\pi}(\psi_1 A_{16} + \psi_2\phi A_{26}) \\ (S_3)_{mn} &= -\frac{m}{\pi}(\psi_1 A_{16} + \psi_2\phi A_{26}) \\ (S_4)_{mn} &= -\frac{n\phi}{\pi}(\psi_1 A_{12} + \psi_2\phi A_{22}) \end{aligned} \tag{D3}$$

whereas $(\tilde{H}_\alpha)_{mn}$ and $(\tilde{I}_\alpha)_{mn}$ are expressed by

$$(\tilde{H}_1)_{mn} = \frac{a\{[(A_{12} + A_{66})d_2 - A_{22}d_1]\lambda_m\mu_n^2 - d_1A_{66}\lambda_m^3 - d_1d_2\lambda_m\}}{\Delta_{mn}} \tag{D4}$$

$$(\tilde{I}_2)_{mn} = \frac{a\{[(A_{12} + A_{66})d_1 - A_{11}d_2]\lambda_m^2\mu_n - d_2A_{66}\lambda_n^3 - d_1d_2\mu_n\}}{\Delta_{mn}} \tag{D5}$$

$$(\tilde{H}_2)_{mn} = 0, \qquad (\tilde{I}_1)_{m,n} = 0 \tag{D6}$$

where

$$\Delta_{mn} = A_{11}A_{66}\lambda_m^4 + (d_2A_{11} + d_1A_{66})\lambda_m^2 + (A_{11}A_{22} - 2A_{12}A_{66} - A_{12}^2)\lambda_m^2\mu_n^2 + (d_1A_{22} + d_2A_{66})\mu_n^2 + A_{22}A_{66}\mu_n^4 + d_1d_2 \tag{D7}$$

Acknowledgment

The authors would like to extend their thanks to the anonymous reviewer for his pertinent comments whose incorporation have resulted in the improvement of the quality of this paper.

References

[1] Vinson, J. R., Rajapakse, Y. D. S., and Carlsson, L. E. (eds.), *Sixth International Conference on Sandwich Structures*, CRC Press, Boca Raton, FL, 2003.

[2] Thomsen, O. T., Bozhevolnaya, E., and Lychegaard, A. (eds.), "Advancing with Sandwich Structures and Materials," *Proceedings of the International Conference on Sandwich Structures*, Springer, New York, 2005.

[3] Mouritz, A. P., Gellert, E., Burchhill, P., and Challis, K., "Review of Advanced Composite Structures for Naval Ships and Submarines," *Composite Structures*, Vol. 53, No. 1, 2001, pp. 21–41.

[4] Vinson, J. R., *The Behavior of Sandwich Structures of Isotropic and Composite Materials*, Technomic Publ., Lancaster, PA, 1991.

[5] Zenkert, D., *An Introduction to Sandwich Construction*, EMAS Publ., Chameleon Press LTD, London, U.K., 1995.

[6] Noor, A. K., Burton, W. S., and Bert, C. W., "Computational Models for Sandwich Plates and Shells," *Applied Mechanics Reviews*, Vol. 49, April 1996, pp. 155–199.

[7] Librescu, L., and Hause, T., "Recent Developments in the Modeling and Behavior of Advanced Sandwich Constructions: A Survey," *Journal of Composite Structures*, Vol. 48, Nos. 1–3, 2000, pp. 1–17.

[8] Vinson, J. R., "Sandwich Structures," *Applied Mechanics Reviews*, Vol. 54, May 2001, pp. 201–214.

[9] Hohe, J., and Librescu, L., "Advanced in the Structural Modeling and Behavior of Sandwich Panels," *Mechanics of Advanced Materials and Structures*, Vol. 11, Nos. 4–5, 2004, pp. 395–424.

[10] Librescu, L., *Elastostatics and Kinetics of Anisotropic and Heterogeneous Shell-Type Structures*, Noordhoff International Publishing, Leyden, The Netherlands, 1975.

[11] Librescu, L., Hause, T., and Camarda, C. J., "Geometrically Nonlinear Theory of Initially Imperfect Sandwich Plates and Shells Incorporating Non-Classical Effects," *AIAA Journal*, Vol. 35, No. 8, 1997, pp. 1393–1403.

[12] Hause, T., Librescu, L., and Camarda, C. J., "Postbuckling of Anisotropy Flat and Doubly-Curved Panels Under Complex Loading Conditions," *International Journal of Solids and Structures*, Vol. 35, No. 23, Aug. 1998, pp. 3007–3038.

[13] Hause, T., Johnson, T. F., and Librescu, L., "Effect of Face-Sheet Anisotropy on Buckling and Post-Buckling of Flat Sandwich Panels," *Journal of Spacecraft and Rockets*, Vol. 37, No. 3, 2000, pp. 331–341.

[14] Gol'denveiser, A. L., *Theory of Elastic Thin Shells*, Pergamon Press, Oxford, England, U.K., 1961.

[15] Leissa, A. W., "Vibration of Shells," NASA, NASA-SP-288, Washington, D.C., 1973, pp. 32, 33.

[16] Qatu, M. S., *Vibration of Laminated Shells and Plates*, Elsevier Acad. Press, New York, 2004, pp. 196–197.

[17] Raville, M. E., and Ueng, C. E. S., "Determination of Natural Frequencies of Vibration of a Sandwich Plate," *Experimental Mechanics*, Vol. 7, No. 4, 1967, pp. 490–493.

[18] Monforton, G. R., and Schmidt, L. A., Jr., "Finite Element Analysis of Sandwich Plates and Cylindrical Shells with Laminate Faces," *Proceedings of the Conference on Matrix Methods on Structural Mechanics*, TR-68-150, Air Force Flight Dynamics Lab., Wright–Patterson Air Force Base, OH, 1968, pp. 573–616.

[19] Zhou, H. B., and Li, G. Y., "Free Vibration Analysis of Sandwich Plates with Laminated Faces Using Spline Finite Point Method," *Computers and Structures*, Vol. 59, No. 2, 1996, pp. 257–263.

[20] Hohe, J., Librescu, L., and Oh, S.-Y., "Dynamic Buckling of Flat and Curved Sandwich Panels with Transversely Compressible Core," *Composite Structures*, Vol. 74, No. 1, 2006, pp. 10–24.

[21] Qatu, M. S., and Leissa, A. W., "Natural Frequencies for Cantilevered Doubly-Curved Laminated Composite Shallow Shells," *Composite Structures*, Vol. 17, No. 3, 1991, pp. 227–256.